


Calcium is not required for triggering volume restoration in hypotonically challenged A549 epithelial cells

Olga Ponomarchuk^{1,2} · Francis Boudreault¹ · Sergei N. Orlov² · Ryszard Grygorczyk^{1,3} 

Received: 22 June 2016 / Revised: 11 September 2016 / Accepted: 14 October 2016 / Published online: 31 October 2016
© Springer-Verlag Berlin Heidelberg 2016

Abstract Maintenance of cell volume is a fundamental housekeeping function in eukaryotic cells. Acute cell swelling activates a regulatory volume decrease (RVD) process with poorly defined volume sensing and intermediate signaling mechanisms. Here, we analyzed the putative role of Ca^{2+} signaling in RVD in single substrate-adherent human lung epithelial A549 cells. Acute cell swelling was induced by perfusion of the flow-through imaging chamber with 50 % hypotonic solution at a defined fluid turnover rate. Changes in cytosolic Ca^{2+} concentration ($[\text{Ca}^{2+}]_i$) and cell volume were monitored simultaneously with ratiometric Fura-2 fluorescence and 3D reconstruction of stereoscopic single-cell images, respectively. Hypotonic challenge caused a progressive swelling peaking at ~20 min and followed, during the next 20 min, by RVD of 60 ± 7 % of the peak volume increase. However, at the rate of swelling used in our experiments, these processes were not accompanied by a measurable increment of $[\text{Ca}^{2+}]_i$. Loading with intracellular Ca^{2+} chelator BAPTA slightly delayed peak of swelling but did not prevent RVD in 82 % of cells. Further, electrophysiology whole-cell patch-clamp experiments showed that BAPTA did not block activation of volume-regulated anion channel (VRAC) measured as

swelling-induced outwardly rectifying 5-nitro-2-(3-phenylpropyl-amino) benzoic acid sensitive current. Together, our data suggest that intracellular Ca^{2+} -mediated signaling is not essential for VRAC activation and subsequent volume restoration in A549 cells.

Keywords VRAC · Osmotic shock · Regulatory volume decrease · Calcium signaling

Introduction

Metazoan cells devoid of contractile vacuoles and lacking rigid cell walls cope with acute hypoosmotic swelling by a compensatory secretion of salt. The main driving force behind this salt secretion derives from the difference between the intracellular chloride electrochemical equilibrium and the cell's resting potential that facilitates chloride efflux. In many cell types, due to elevated resting membrane permeability to potassium, chloride efflux is accompanied by efflux of K^+ as a counterion. Therefore, a sole increase in anion permeability, through activation of volume-regulated anion channel (VRAC), is thought sufficient to elicit the volume restoration process [21, 30]. Several aspects of this regulatory volume decrease (RVD) remain undefined; however, notably how VRAC is activated by cell swelling. Lack of consensus concerning the molecular identity of VRAC proteins certainly stalled the progress in this knowledge area [21]. The recent identification of a candidate for VRAC, the multipass transmembrane leucine-rich binding motif LRRC8 protein [39, 51], with 5 paralogs in chordates LRRC8A, B, C, D, and E [1], can thus be seen as a positive development [30, 36]. Several mechanistic aspects of RVD remain incompletely understood; however, most notable is the precise role of intracellular calcium signaling. Indeed, acute and rapid changes in

✉ Francis Boudreault
francis.boudreault.crchum@gmail.com

✉ Ryszard Grygorczyk
ryszard.grygorczyk@umontreal.ca

¹ Centre de recherche, Centre hospitalier de l'Université de Montréal (CRCHUM), Tour Viger 900 rue St-Denis, Montreal, Quebec H2X 0A9, Canada

² Faculty of Biology, M.V. Lomonosov Moscow State University, Moscow, Russia

³ Department of Medicine, Université de Montréal, Montreal, Quebec, Canada

extracellular tonicity is often accompanied by elevation of $[Ca^{2+}]_i$ in several cell types including human lung carcinoma A549 cells [8], cervical cancer cells [43], rat lacrimal acinar cells [47], primary astrocyte cultures [34], and Ehrlich ascites tumor cells [37]. Albeit several studies have shown those hypo-induced calcium responses to control and regulate the subsequent RVD [21, 28, 35], others minimized $[Ca^{2+}]_i$ involvement to a strictly permissive role, for example, in Ehrlich mouse ascites tumor cells [23] and bovine chromaffin cells [14].

Because hypo-induced $[Ca^{2+}]_i$ responses differ not only between cell type but also within a single cell population [8], [28], better understanding of the involved processes requires single-cell level simultaneous measurement capabilities of both variables—cell volume and $[Ca^{2+}]_i$. Current approaches to assess volume restoration based on high-throughput techniques, such as commercially available Coulter-counter [10], do not meet this requirement. Custom-designed techniques to track the volume of a single cell had been satisfactorily employed, yet they also have limitations [4]. For instance, volume is determined either through proxies, such as monitoring isosbestic fluorescence level [4, 7] or quantified with invasive technique employing high-energy light-source, e.g., confocal microscopy [40]. Although the recent development of a digital holographic microscopy could allow non-invasive determination of volume and morphology of larger number of individual cells [13], this approach has currently no capacity for simultaneous monitoring of intracellular $[Ca^{2+}]_i$.

Keeping in mind the above limitations, we adapted our previously described, light microscopy-based, and non-invasive stereoscopic technique [9, 17] to simultaneously quantify alteration in volume and $[Ca^{2+}]_i$ within single substrate-adherent cells. VRAC currents were also measured at the single-cell level in parallel patch-clamp experiments. Hypotonically challenged A549 cells analyzed with this approach revealed that intracellular Ca^{2+} -mediated signaling is not obligatory for VRAC activation and subsequent cell volume restoration.

Materials and methods

Cells

Human lung carcinoma A549 cells were grown at 37 °C in Dulbecco's modified Eagle's medium (DMEM) supplemented with 10 % fetal bovine serum (FBS), 2 mM L-glutamine, 50 U/ml penicillin-G, and 50 µg/ml streptomycin sulfate in a 5 % CO₂. For volume and calcium measurements, cells were seeded on 25-mm diameter glass coverslips at ~10 cells/mm² concentration in low-serum (0.1–0.5 % FBS) growth medium. Cells were used 24–72 h after plating. For electrophysiology experiments, cells were seeded on 15-mm glass coverslips

(~10 cells/mm²) in 10 % FBS-containing DMEM growth medium which did not include L-glutamine and antibiotics. Cells were used in patch-clamp experiments 36–72 h later. Culture media was from HyClone (Logan, UT) and all added constituents were from Gibco/Thermo Fisher Scientific (Burlington, ON).

Microscopy setup for simultaneous fluorescence microscopy and cell volume

To track volume changes, A549 cells were mounted in a modified version of a custom-designed side-view chamber previously described in [9], but here with larger internal dimensions (5 × 10 × 25 mm³), and placed on the stage of a NIKON TE300 inverted microscope equipped with epifluorescence UV illumination (Nikon Canada Inc., Mississauga, ON). During experiments, cells were continuously perfused with warm (37 °C) solution using a peristaltic pump (Gilson, Middleton, WI) at rate of ~0.5 ml/min. After equilibration in physiological isotonic solution (IS) (see the “Solutions and chemicals” section) for at least 15 min, the cells were challenged with ~50 % hypotonic solution (HS) for up to 45 min. A half-size version (5 × 5 × 25 mm³) of this chamber with increased fluid turnover rate and faster cell swelling rate was also employed for some calcium measurements (see Fura-2-based calcium measurements).

Cell volume was measured with an improved version of the DISUR technique [17]. The method involves 3D reconstruction of cell shape based on two light microscopy images acquired at perpendicular directions. Side-view and top-view images were captured with two miniature, charge-coupled cameras (Moticam 352, Motic Instruments Inc., Richmond, BC; mvBlueFOX, Matrix Vision, Oppenweiler, Germany), every each 15 s. The images served to generate a set of topographical curves of the cell surface from its digitized (spline function) side-view profile and base outline. Cell volume was calculated from the reconstructed cell topographical model with MATLAB (MathWorks, Inc., Natick, MA).

During simultaneous calcium and volume measurements, side-view images were continuously recorded together with fluorescence measurements. To prevent dye photobleaching, as well as cross-talk between transmitted light images and fluorescence images, we used a 645-nm (red) long-pass filter (Thorlabs, Newton, NJ). Because cell base outline is minimally affected during moderate cell swelling, top-view images were acquired at 5-min interval, in contrast to side-view images that were acquired at 15-s interval.

Fura-2-based calcium measurements

To load Fura-2, A549 cells were incubated (1 h, 37 °C, 5 % CO₂) in phenol red-free medium DMEM/F-12 (1:1) (HyClone, Logan, UT) containing 10 µM Fura-2-AM. Cells

were then equilibrated 30 min in DMEM/F-12 (1:1). For calcium imaging, the cells were exposed to alternate (300 ms) 340/380 nm illumination from a high-pressure mercury lamp (100 W, Osram GmbH, Germany) via interference filters (Chroma Technology, Brattleboro, VT) mounted on a filter wheel (Sutter Lambda 10-C, Sutter Instrument, Novato, CA). Fluorescence images were recorded at 15-s intervals with a MicroMAX digital camera (Princeton Instruments Inc., Trenton, NJ) and stored for later analysis. As a positive control for Ca^{2+} detection 10 μM ionomycin, a Ca^{2+} ionophore was applied at the end of experiment. Changes of $[\text{Ca}^{2+}]_i$ are shown as Fura-2 fluorescence F_{340}/F_{380} ratio normalized to that before cell stimulation.

BAPTA loading

To chelate intracellular Ca^{2+} , cells were loaded with BAPTA in phenol red-free medium DMEM/F-12 (1:1), containing 10 μM BAPTA-AM for 1.5 h (37 °C, 5 % CO_2). This procedure has been previously used to suppress the elevation of $[\text{Ca}^{2+}]_i$ in hypotonically challenged A549 cells [49].

Electrophysiology

For whole-cell patch-clamp experiments, A549 cells were plated at low density (~ 10 cells/ mm^2) on 15-mm diameter glass coverslips. Patch pipettes, made from borosilicate glass (A-M Systems, Inc. Sequim, WA), were filled with (mM): 100 CsCl, 90 sorbitol, 2 MgCl_2 , 1 EGTA, 1 MgATP , and 10 TES, pH 7.4 (Tris) (304 mOsm/kg H_2O). MgATP (from 100 mM stock) was added to the solution on the day of experiment. For BAPTA experiments, 10 mM BAPTA-Cs (Toronto Research Chemicals Inc., Toronto, ON) was added and sorbitol lowered to 65 mM (Osmolarity 298 mOsm/kg H_2O). BAPTA use was warranted for its superior calcium selectivity and faster binding kinetics compared to EGTA [12]. With 10 mM BAPTA, the free Ca^{2+} concentration will be clamped well below the 1 nM range (≤ 0.4 nM; MAXchelator, 10 mM EGTA, 10 μM Ca, pH 7.0, 0.3 N ionic strength, $t = 37$ °C). Whole-cell currents were measured at room temperature with an Axopatch 200B amplifier (Axon instruments, Molecular Devices, Sunnyvale, CA). Current responses to the computer-generated stimulus waveform were filtered at 2 kHz, digitized (Digidata 1200, Molecular Devices) at 1 kHz, and recorded on computer by Clampex 8.2 software. The data were analyzed offline by pCLAMP 8 software (Molecular Devices). Acute 50 % hypotonic shock was achieved by adding appropriate amounts of 98 % hypotonic solution (containing only 1 mM MgCl_2 and 1 mM CaCl_2) to the bath filled with isotonic physiological solution (IS).

Solutions and chemicals

Physiological isotonic solution (IS) contained (mM) the following: 140 NaCl, 5 KCl, 1 MgCl_2 , 1 CaCl_2 , 10 glucose, and 10 HEPES, pH 7.4, adjusted with NaOH. Hypotonic solution (HS) was prepared by reducing salt concentration while keeping divalent cation concentration constant (mM): 1 MgCl_2 and 1 CaCl_2 . For nominally extracellular calcium-free solution (0 mM $[\text{Ca}^{2+}]_o$), calcium was replaced mole-for-mole with magnesium. The osmolarity was measured with a freezing point osmometer (Micro Osmometer 3320, Advanced Instruments Inc., Norwood, MA) at 309 mOsm/kg H_2O for IS and 161 mOsm/kg H_2O for HS. Stocks of Fura-2 AM, ionomycin, BAPTA-AM, and 5-nitro-2-(3-phenylpropylamino) benzoic acid (NPPB) were prepared in DMSO at concentrations of 2, 1, 25, and 100 mM, respectively. MgATP (100 mM) was dissolved in water. Reagents were from Fisher Scientific (Pittsburgh, PA) (MgCl_2 , CaCl_2 , KCl); ACP Chemicals Inc. (Montreal, QC) (NaCl, NaOH); BioShop Canada Inc. (Burlington, ON) (HEPES); Invitrogen/Thermo Fisher Scientific (Burlington, ON) (Tris); Bio Basic Canada Inc. (Markham, ON) (EGTA). Molecular Probes, Invitrogen Corp. (Burlington, ON, Canada) (Fura-2 AM, BAPTA-AM). Otherwise, reagents were from Sigma-Aldrich Canada Co (Oakville, ON).

Results

Time-course of hypotonic cell swelling

When cells are exposed to hypotonic solution by perfusion, rate of cell swelling will depend on the rate at which tonicity will change inside the imaging chamber as dictated by the fluid turnover (fluid exchange) rate, i.e., Q/V , where Q is a fluid flow rate (ml/min) and V is a chamber internal volume. To assess the impact of fluid turnover on cell swelling kinetics in our experimental setup, theoretical changes in swelling time-course (not including VRAC activation) were simulated with a single exponential fluid tonicity decay model (Eq. 1) and plasma membrane permeability parameters derived from [8, 15, 19]. The simulated cell volume time-course was calculated with Eqs. 1-4 coded into an iterative loop with incremental time δt . Figure 1 depicts the impact of increasing chamber volume (decreasing fluid turnover rate) on cell swelling kinetics. Note the augmented time to reach maximal volume with chambers of slower fluid turnover rate:

$$C_{\text{chamber}_i} = C_{\text{inflow}} + (C_{\text{chamber}_0} - C_{\text{inflow}}) e^{-\left(\frac{Q \cdot \delta t}{V_{\text{chamber}}}\right)} \quad (1)$$

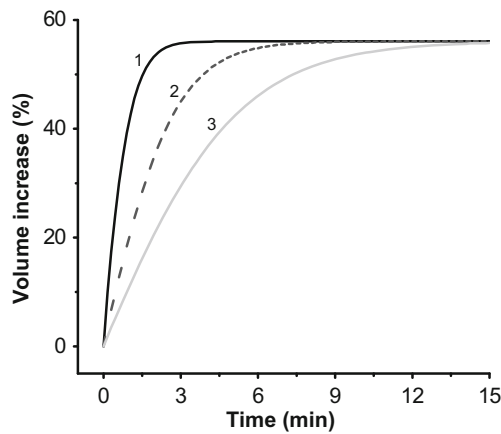


Fig. 1 Impact of fluid turnover rate on hypotonicity-induced cell swelling kinetics. Chamber size will affect fluid turnover and cell swelling kinetics during application of hypotonic solution perfused at a fixed flow rate. Cell swelling time-course was simulated with a single exponential fluid tonicity decay model (Eq. 1), for perfusion rate Q of 0.5 ml/min and different chamber volume V of 0.2, 0.625, or 1.25 ml, corresponding to fluid turnover of 2.5, 0.8, and 0.4 min^{-1} , respectively, curves 1 through 3. Parameters were as follows: C_{inflow} (solute concentration of flowing solution) = 161 mOsm/L; C_{chamber_0} (initial osmotically active solute concentration inside the chamber) = 309 mOsm/L; $Q = 0.5$ mL/min; C_{cytosol_0} (initial osmotically active solute concentration within cell) = 309 mOsm/L; V_0 (initial cell volume) = 5 pL; R (Ponder's value) = 0.61; V_w (partial molar volume of water) = $1.8 \cdot 10^{-5}$ m^3/mol ; P_f (normalized plasma membrane osmotic water permeability) = $2.2 \cdot 10^{-5}$ m/s; S (cell surface) = $3000 \mu\text{m}^2$; $\delta t = 10$ s

$$C_{\text{cytosol}_i} = C_{\text{cytosol}_0} * \frac{V_0 * R}{V_{i-1} - (1-R) * V_0} \quad (2)$$

$$\Delta C_i = C_{\text{cytosol}_i} - C_{\text{chamber}_i} \quad (3)$$

$$V_i = V_{i-1} + V_w * P_f * S * \Delta C_i * \delta t \quad (4)$$

The actual experimentally observed time-course of hypotonic cell swelling observed at fluid turnover rate of $\sim 0.4 \text{ min}^{-1}$ is depicted in Fig. 2a. It shows that perfusate of reduced tonicity evoked a progressive cell swelling peaking around 22 ± 2 min with volume increase reaching $40 \pm 6\%$ (V_{max}) and declining asymptotically toward prestress volume. Volume restoration 20 min after maximum swelling (VR_{20}) was $60 \pm 7\%$ of the peak volume increase. Such pace of hypo-induced swelling is moderate in comparison with similar experiments where faster fluid turnover was used, and maximal volume was attained in shorter period of time, e.g., ~ 2.5 to 5 min [8]. This results from design trade-off between imaging requirements and chamber size, leading to improved quality of images at the expense of diminished fluid turnover rate for chamber of larger volume, hence the slower swelling. Nevertheless, in this study, A549 cells swelled to volume comparable to that reported earlier [49], where cells were experiencing faster swelling. Importantly, slower swelling did not affect RVD in our experiments, which proceeded typically as previously reported [21].

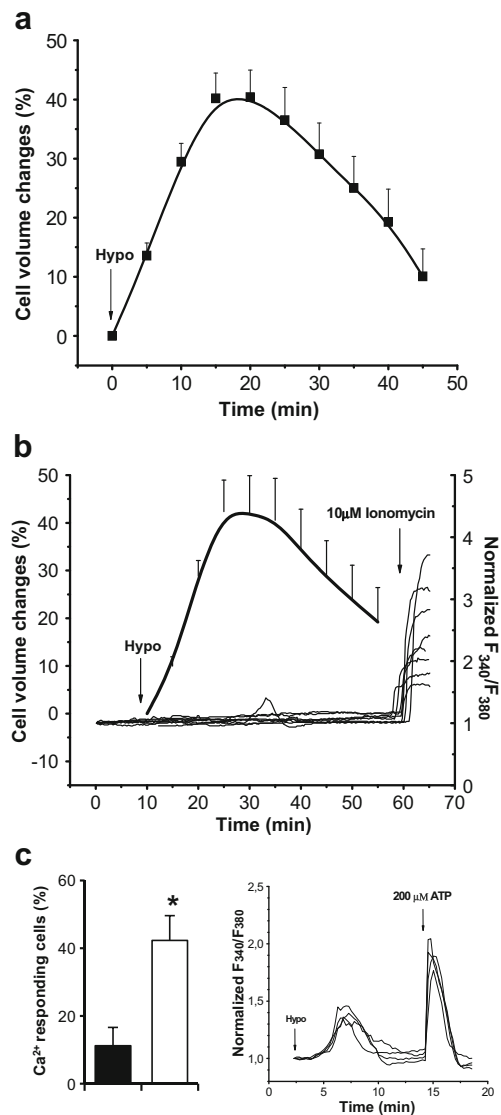


Fig. 2 Cell volume changes in response to 50 % hypotonic shock. **a** Average kinetics of cell volume changes caused by 50 % hypotonic challenge in control A549 cells observed at fluid turnover rate Q/V of $\sim 0.4 \text{ min}^{-1}$. Data are presented as mean \pm SEM ($n = 17$). Data plot shows relative volume normalized to cell volume at the start of swelling. **b** Hypotonicity-induced $[\text{Ca}^{2+}]_i$ changes (shown as normalized F_{340}/F_{380} ratio) and volumes changes measured simultaneously in Fura-2-loaded A549 cells. Kinetics of $[\text{Ca}^{2+}]_i$ changes in single cells ($n = 7$, thin line curves) and average kinetics of volume changes (mean \pm SEM, $n = 11$, thick line) are presented. Data plots show relative volume normalized to cell volume at the start of swelling. **c** Swelling-induced calcium responses are diminished at slower fluid turnover rate in the imaging chamber. A549 cells were tonically swelled with 50 % hypotonic solution applied by continuous perfusion at a flow rate of 0.5 ml/min. Percentage of calcium-responsive cells were counted per field of view for two different fluid turnover rates of 0.4 and 0.8 min^{-1} , black and white bar respectively; corresponding chamber volumes were 1.25 ml ($n = 6$) (regular) and 0.625 ml ($n = 6$) (reduced). In chamber with reduced size, percentage of responding cells was significantly higher. Data are presented as mean \pm SEM, *Statistically significant difference ($p < 0.05$, Student's t test). Examples of hypo-induced $[\text{Ca}^{2+}]_i$ responses observed with a smaller volume chamber are shown on the right

Calcium and RVD

Having established the cell swelling kinetics and occurrence of RVD, we then verified how $[Ca^{2+}]_i$ level varies during the hypotonic challenge. Under similar experimental conditions, except the cytosolic inclusion of calcium-detecting dye Fura-2, A549 cells duly demonstrated almost identical volume expansion and shrinkage kinetics (Fig. 2b) as in the absence of Fura-2. In contrast, $[Ca^{2+}]_i$ behaved unexpectedly. Cells did not show noticeable variation in $[Ca^{2+}]_i$ during swelling phase nor after initiation of RVD, despite a robust ionomycin response which demonstrated that cells were readily responsive to $[Ca^{2+}]_i$ changes. We attributed the absence of measurable $[Ca^{2+}]_i$ responses, except few minor probably spontaneous fluctuations, to slower cell swelling kinetics as discussed above. Indeed, faster cell expansion rates have been associated with stronger calcium responses in previous studies [8, 29].

In support to this finding, we analyzed the calcium response of a larger population of cells (confluency at the time of experiments ~ 300 cells/mm²). Only $11 \pm 5\%$ cells ($n = 6$ independent experiments) presented a detectable increase in $[Ca^{2+}]_i$ at the fluid turnover rate of ~ 0.4 min⁻¹ used in these experiments. In contrast, decreasing by approximately half the volume of the chamber, and thus increasing the fluid exchange rate to ~ 0.8 min⁻¹ and hence pace of cell swelling, nearly quadrupled ($42 \pm 7\%$, $n = 6$) the number of positively responsive cells (Fig. 2c). It further demonstrates the association between the rate of the hypotonic shock application, cell swelling pace, and the $[Ca^{2+}]_i$ response. Considering the low number of responding cells observed at lower fluid exchange rate, the odds of randomly selecting a calcium-responsive cell for volume reconstruction was thus small, and readily explained lack of $[Ca^{2+}]_i$ responses in experiments depicted in Fig. 2b.

Clearly, the undiminished volume restoration in the absence of appreciable changes in $[Ca^{2+}]_i$ undermines the idea that calcium acts as an important second messenger during RVD in A549 cells. Yet, localized calcium signaling within subcellular regions or contiguous to plasma membrane targeting nearby channels and/or receptors have been documented [50] and may have gone undetected in our Fura-2 fluorescence assay. Thus, to further rule out a possible implication of local $[Ca^{2+}]_i$ elevations in RVD, we resorted to BAPTA, a highly specific and fast-acting calcium chelator [12]. BAPTA-loaded A549 cells presented slightly altered morphology with diminished spreading; nevertheless, they withstood the hypotonic stress without detaching from the substrate. Figure 3a shows that $[Ca^{2+}]_i$ chelation slightly dampened the speed of both swelling and RVD. Though this dampening effect did not pass the *t* test (Fig. 3b), it remained intriguing and of concern, especially in the light of the suggested role of calcium in regulation of VRAC activity, whether acting as a turn-on switch [5] or more likely as a permissive

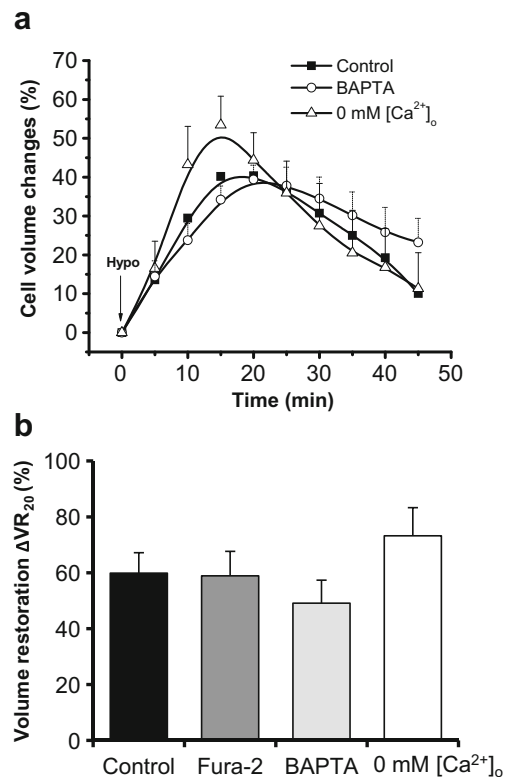


Fig. 3 Impact of Ca^{2+} manipulation on cell swelling and RVD. **a** Average kinetics of cell volume changes (%) caused by 50 % hypotonic challenge in control A549 cells ($n = 17$, closed squares), cells loaded with BAPTA ($n = 11$, open circles), and 0 mM $[Ca^{2+}]_o$ ($n = 5$, open triangles). Average kinetic data for BAPTA-loaded cells and 0 mM $[Ca^{2+}]_o$ are presented as mean \pm SEM. Data plots show relative cell volume normalized to volume at the start of swelling. **b** RVD response was quantified as percentage of volume restoration 20 min after reaching maximal swelling (ΔVR_{20}). The graph shows ΔVR_{20} for control A549 cells ($n = 17$), A549 cells loaded with Fura-2 ($n = 11$) or with BAPTA ($n = 11$), and cells under nominally free extracellular calcium (0 mM $[Ca^{2+}]_o$, $n = 5$) during 50 % hypotonic challenge. Data are presented as mean \pm SEM. No statistically significant differences were observed for all three conditions compared to control (Student's *t* test)

signal [48]. In short, clamping $[Ca^{2+}]_i$ at low ($\sim 10^{-9}$ M) level only slightly slowed down the RVD suggesting minimal impact on VRAC activity. Finally, the removal of extracellular calcium did not impact the rate of volume restoration (Fig. 3a, b) thus implying that only calcium of intracellular origin (e.g., from calcium stores) could minimally affect VRAC.

Calcium and VRAC

To test directly whether VRAC activity depends on $[Ca^{2+}]_i$ and in keeping with our single-cell approach throughout the study, we used the whole cell patch-clamp technique. To block K^+ currents, patch pipettes were filled with CsCl solution (see the “Methods” section). In a representative experiment illustrated in Fig. 4, volume-sensitive current developed few minutes after diluting the extracellular bathing milieu down to $\sim 50\%$ of normal tonicity, while keeping divalent cation Ca^{2+}

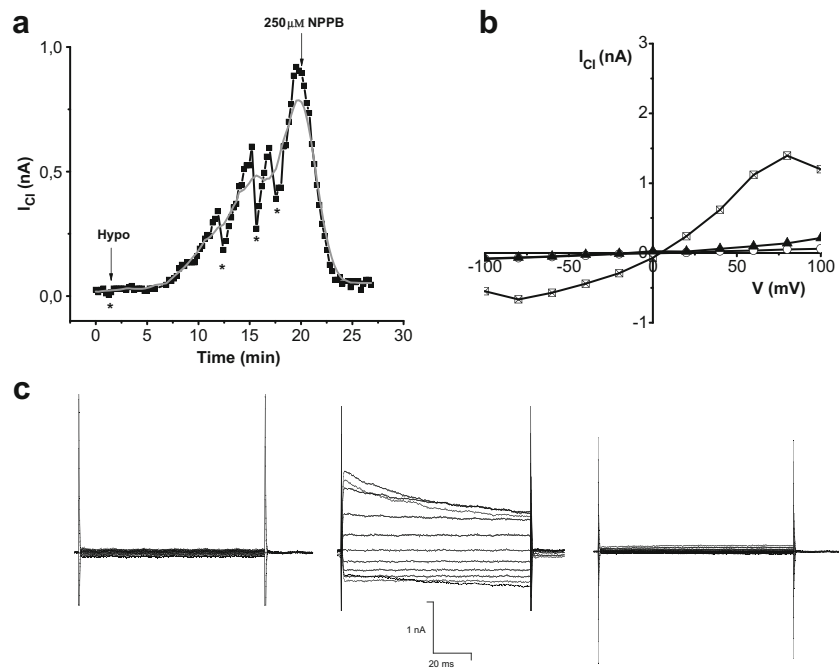


Fig. 4 Swelling-induced whole-cell currents in A549 cells. **a** Time-course of whole-cell voltage-clamp currents recorded every 15 s in response to 100-ms pulses from 0 to 40 mV before and after application of 50 % hypotonic shock. Cell swelling-induced current was rapidly blocked by the NPPB (250 μ M). *Time points where current-voltage (I-V) relationship was determined, such as those shown in **b** and **c**, producing small perturbations on the current time-course curve. **b** I-V plots under isotonic condition (IS solution, *open circle*), 50 % hypotonic shock

(*open squares*), and 50 % hypotonic shock + NPPB (*solid triangles*). I-V relationship measured at the beginning of the voltage steps displays typical outward rectification as expected for volume-sensitive current. **c** Whole-cell currents in response to voltage steps between -100 and $+100$ mV in 20-mV increments delivered from a holding voltage of 0 mV under (from left to right): isotonic condition, 50 % hypotonic shock, and 50 % hypotonic shock + NPPB. Pipette contained CsCl solution while bath IS or HS solution (see the “Methods” section)

and Mg^{2+} concentration constant. Acute addition of a Cl^- channel blocker NPPB (250 μ M) to the bath quickly blocked the rising plasmalemmal permeability (Fig. 4a) and confirmed that developing current came from anionic channels, presumably VRAC. Further indication of VRAC activation comes from the pronounced outward rectification (Fig. 4b) and slight current deactivation observed at high depolarizing voltages (Fig. 4c, middle panel), which are considered typical of volume-sensitive current mediated by VRAC. We repeated those experiments with 10 mM BAPTA included in the pipette solution (Fig. 5). After getting access to the cytosol in the whole-cell patch-clamp configuration, the internal diffusion of such high BAPTA concentration will clamp $[Ca^{2+}]_i$ well below the 1 nM range (≤ 0.4 nM). This effectively abolishes intracellular calcium ion activity in the patched cell. Surprisingly, neither the kinetics nor the amplitude of the volume-sensitive chloride current was negatively affected by the intracellular BAPTA (Fig. 5). Outward rectification, NPPB block, and deactivation at elevated depolarizing voltage, all signature features of VRAC, remained similar as in the control cells shown on Fig. 4.

A549 volume-sensitive currents once activated rarely plateaued in our hands: a steady exponential-like increase

was predominantly observed until loss of cell integrity, presumably as a result of excessive swelling due to continuous cell dialysis with the isotonic CsCl solution in the pipette and block of K^+ permeability by Cs^+ . In consequence, we compared NPPB-sensitive and outwardly-rectifying current after 7 min of activation in BAPTA-loaded cells against control. It showed that while intracellular calcium chelation negligibly slowed down rate of cell swelling (Fig. 3a), it potentiated (doubled) the volume-sensitive current (Fig. 5d) at that time point, thus plainly demonstrating that calcium itself, or via its associated signaling pathways, has no positive impact on VRAC activation.

LRRC8 proteins

The identity of VRAC remained a contentious issue for years, but the latest identification of LRRC8 as VRAC channel-forming or associated proteins, identified through high-throughput siRNA-based assay, revealed a very promising new candidate [39, 51]. According to our observations reported here, this novel candidate should bear very few calcium-related functional domains. Thus, further proof that LRRC8 forms VRAC or closely regulate VRAC shall come from the

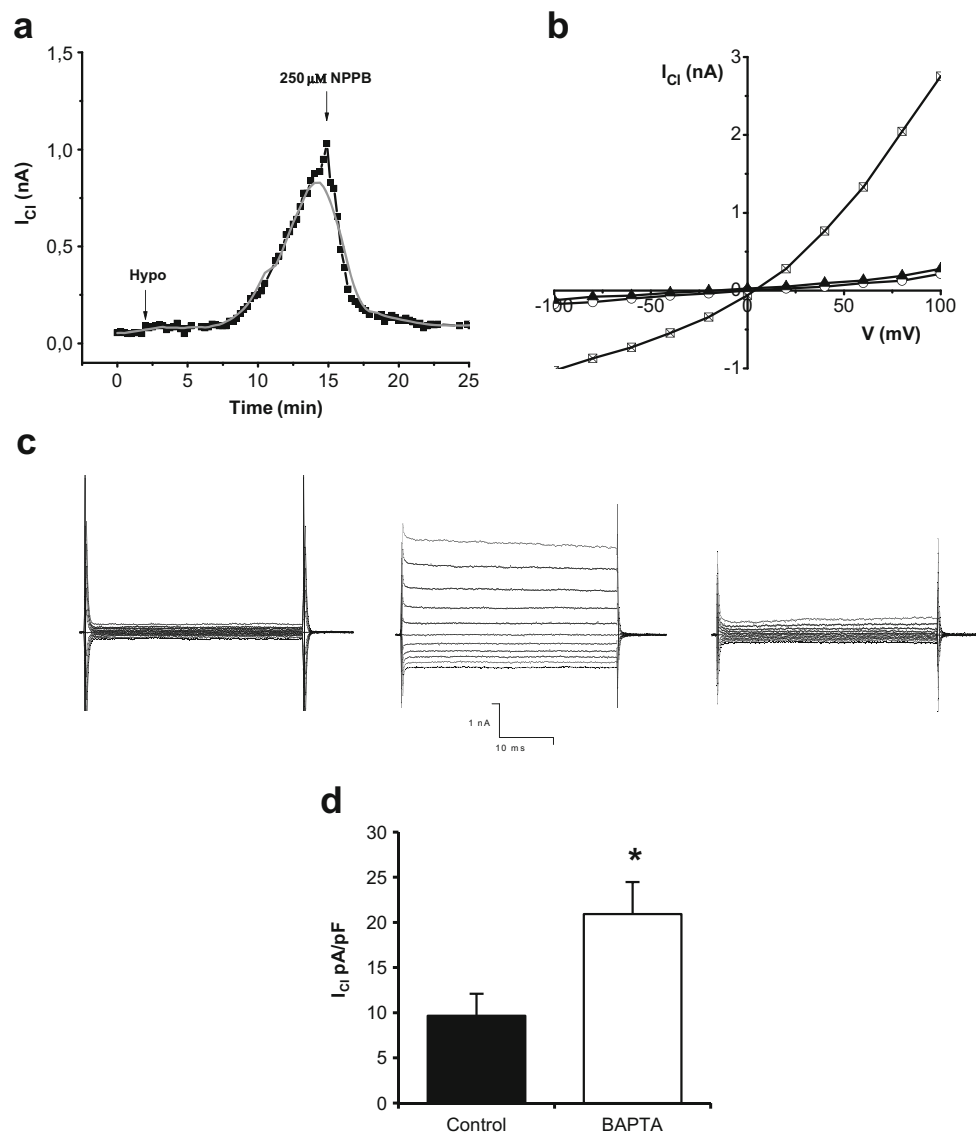


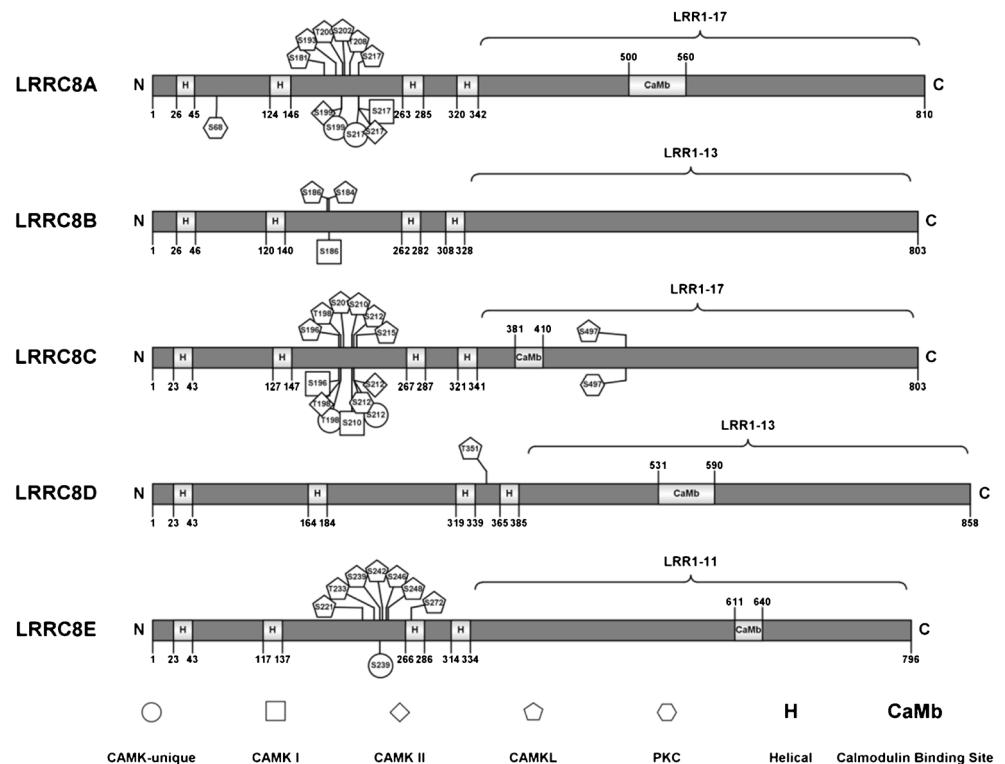
Fig. 5 Swelling-induced whole-cell currents in BAPTA-loaded A549 cells. **a** Whole-cell patch-clamp experiments were performed on A549 cells with 10 mM BAPTA in the pipette solution. Currents were recorded every 15 s in response to alternate 100-ms pulses from 0 to 40 mV. NPPB abolished the volume-sensitive current. **b** I-V plots under isotonic condition (IS solution, *open circles*), 50 % hypotonic shock (*open squares*), and 50 % hypotonic shock + NPPB (*solid triangles*). **c** Whole-cell currents in response to voltage steps between -100 and $+100$ mV in 20-mV increments delivered

from a holding voltage of 0 mV under (from left to right) isotonic condition, 50 % hypotonic shock, and 50 % hypotonic shock + block of VRAC with NPPB. Pipette contained CsCl solution while bath IS or HS solution (see the “Methods” section). **d** NPPB sensitive outwardly rectifying current in control and BAPTA-loaded cells, *black* and *white* bar respectively. Currents were measured 7 min after hypotonic challenge in control ($n = 6$) and BAPTA ($n = 4$); experiments are presented as mean \pm SEM, *Statistically significant difference ($p < 0.05$, Student’s t test)

absence or minimal presence of any calcium-dependent domain in its molecular composition. We therefore analyzed its amino acid sequences, as listed on UniProt website (<http://www.uniprot.org/>, (UniProt 2015)) with either web-based applications (Calmodulin Target Database, <http://calcium.uhnres.utoronto.ca/>) [52] or visual alignment with well-known calcium-related consensus sequences as reported in the literature (<http://calcium.uhnres.utoronto.ca/>;

<http://www.uniprot.org/>) and selected only curated phosphorylation site as reported on PhosphoSitePlus® (<http://www.phosphosite.org/> [22]). LRRC8 family protein analysis for Ca^{2+} /calmodulin binding sites and Ca^{2+} /calmodulin phosphorylation sites is shown in Fig. 6; diagrams were produced by using IBS software (Version 1.0), [27]. It shows that all LRCC8 paralogs bear several amino acid sequences known to potentially interact either directly with calmodulin or

Fig. 6 Domain analysis of LRRC8 proteins. LRRC8 family protein analysis for Ca^{2+} /calmodulin binding sites and Ca^{2+} /calmodulin phosphorylation sites. Abbreviations: *CaM* binding Ca^{2+} /calmodulin binding site, *CAMK-unique* Ca^{2+} /calmodulin-dependent protein kinase-unique, *CAMKI* Ca^{2+} /calmodulin-dependent protein kinase I, *CAMKII* Ca^{2+} /calmodulin-dependent protein kinase II, *CAMKL* Ca^{2+} /calmodulin-dependent protein kinase-like, *PKC* protein kinase C



to form a phosphorylation target for well-known Ca^{2+} -dependent kinases such as CAMKI, CAMKII, or PKC. Our analysis is in line with previous report based on sequence homology [1] foreseeing a strong calcium relationship for LRCC8a inferred from Pannexin homologies. Of course, whether those sequences are truly functional domains and, more importantly, whether those putative domains are involved in the activation or gating mechanisms of VRAC remains to be shown. In any case, our findings reported here do not support the notion that in A549 cells and under our experimental conditions, these domains are involved in triggering or maintaining VRAC activity but instead they may exert a negative VRAC modulation.

Discussion

In this study, we investigated the relationship between swelling-induced RVD occurrence, $[\text{Ca}^{2+}]_i$ signaling, and VRAC activation in A549 cells by performing simultaneous measurements of cell volume and $[\text{Ca}^{2+}]_i$ changes in single cells. This was complemented by parallel patch-clamp whole-cell recordings of VRAC-mediated current. We found that intracellular Ca^{2+} signaling is not essential for VRAC activation and subsequent cell volume restoration.

The prevalence of $[\text{Ca}^{2+}]_i$ fluctuations in hypotonically challenged cells reported in several previous studies naturally

led to the suggestion that osmotically triggered RVD could depend on calcium signaling [6, 10, 21, 42, 47]. Our present findings in a model epithelial A549 cells, however, clearly demonstrated the co-incidental nature of hypo-induced calcium fluctuations and triggering of RVD. This is based on three major observations. First, under moderate rate of swelling, A549 cells rarely experience $[\text{Ca}^{2+}]_i$ variations, yet they normally restore their volume. Second, pharmacological blocking of calcium signaling did not prevent RVD, though we noticed a somewhat depressed pace of volume recovery. Finally, VRAC-mediated currents were not attenuated in the presence of intracellular BAPTA; on the contrary, we observed a significant augmentation of VRAC current measured 7 min after hypotonic challenge.

Our findings are consistent with earlier reports indicating that $[\text{Ca}^{2+}]_i$ increase is not required for VRAC activation and/or completion of RVD [47]. They are, however, at variance with reports indicating that $[\text{Ca}^{2+}]_i$ of ~ 50 nM is needed for VRAC activation [48] or it has a permissive role as reported for HeLa cells where VRAC activity was inhibited with calmodulin antagonists [11, 24]. Surprisingly, in our patch-clamp experiments, when $[\text{Ca}^{2+}]_i$ was kept below ~ 1 nM, thereby knocking off most if not all possible protein-calcium interactions in the cell, VRAC currents were in fact enhanced, demonstrating the negative modulation of VRAC activity by calcium. Therefore, moderate diminution of RVD rate in BAPTA-loaded cells requires an alternate explanation.

Cytoskeleton remodeling, such as that occurring during cell swelling, mobilizes multiple signaling pathways, notably Rho-ROCK, RAC1, and CDC42 with calcium signaling pathways restricted to a peripheral yet at times of important role in this process [45]. Our results demonstrate that strong calcium buffering does not stop osmo-swollen cells to return to their former volume, but it slows down the pace of recovery. A sluggish RVD was also observed, albeit to a lesser extent, in Fura-2-loaded cells perhaps as a result of mild buffering by the calcium-sensitive dye [47] or damages by UV-ray exposure. Cytoskeleton reorganization is also temperature-sensitive [33] and so is RVD [38]. Considering that VRAC current develops promptly at RT, whereas RVD shows varying signs of impairment at this temperature [46], indicates that stimulation of volume-sensitive current alone does not suffice to induce cell shrinkage, implicating cytoskeleton as a possible temperature and Ca^{2+} -sensitive component of the RVD process. Thus, our single-cell based study suggests $[\text{Ca}^{2+}]_i$ involvement in the RVD likely via cytoskeleton remodeling with no role, even a permissive one [48], in VRAC activation or its steady-state activity. It should be noted that other factors may have also caused slower RVD in BAPTA-loaded cells, for instance, Ca^{2+} -activated K^+ channel might have contributed to RVD [35] and have experienced reduced activity, thereby reducing the rate of net KCl efflux.

A wide range of proteins/enzymes and ion channels, including K_{Ca} and Cl_{Ca} channels, depend on $[\text{Ca}^{2+}]_i$ for their activation or modulation [26]. For a time, Cl_{Ca} channels had even been proposed as candidate to mediate VRAC current. Although this idea has fallen out of favor [25, 44], it highlights a possible interplay between RVD and hypo-induced $[\text{Ca}^{2+}]_i$ fluctuations via calcium or Ca^{2+} -dependent effectors observed in several cells and experimental models [16, 20, 32, 41]. In some cell type, VRAC current activity and VRAC-mediated organic osmolyte release can be stimulated or potentiated with $[\text{Ca}^{2+}]_i$ -associated GPCR activation alone or in combination with moderate cell swelling [2, 3, 31]. Our present study, however, does not support the notion of $[\text{Ca}^{2+}]_i$ involvement in VRAC activation of acutely swollen A549 cells. The latest identification of LRRC8 proteins as either forming VRAC or closely regulating its activity [39, 51] is a major step forward toward elucidating the molecular mechanisms orchestrating RVD. In light of our findings, LRRC8s proteins shall present little affinity to calcium or calcium-associated proteins when it comes to gating mechanisms or regulation. Intriguingly, our computer-based AA sequence analysis revealed several calcium-related domains within LRRC8. This finding coupled with our observation that BAPTA potentiates VRAC current in our A549 cells indicates, though counterintuitively, a negative modulatory role for $[\text{Ca}^{2+}]_i$.

Deciphering intracellular signaling pathways that control cell volume restoration has barely begun and several important questions remain unanswered, including mechanisms of

VRAC activation and regulation, cytoskeleton reorganization, and most notably, the volume sensor identity. Whether the latter is a single entity, or protein, or multiscale scaffolding remains to be determined. Calcium as second messenger now seems a very minor component in this mechanosensitive signaling, but several other molecules have been proposed though none made consensus yet [21]. The pathways orchestrating the volume restoration remain an uncharted territory for most part, but concepts such as macromolecular crowding [53] and cytoplasmic hydrogel behavior [18] will serve as resourceful guides along the way.

Acknowledgments This study was supported by Natural Science and Engineering Research Council of Canada discovery grant RGPIN 435517-2013 (RG).

References

1. Abascal F, Zardoya R (2012) LRRC8 proteins share a common ancestor with pannexins, and may form hexameric channels involved in cell-cell communication. *BioEssays* 34:551–560
2. Akita T, Fedorovich SV, Okada Y (2011) Ca^{2+} nanodomain-mediated component of swelling-induced volume-sensitive outwardly rectifying anion current triggered by autocrine action of ATP in mouse astrocytes. *Cell Physiol Biochem* 28:1181–1190
3. Akita T, Okada Y (2011) Regulation of bradykinin-induced activation of volume-sensitive outwardly rectifying anion channels by Ca^{2+} nanodomains in mouse astrocytes. *J Physiol* 589:3909–3927
4. Altamirano J, Brodwick MS, Alvarez-Leefmans FJ (1998) Regulatory volume decrease and intracellular Ca^{2+} in murine neuroblastoma cells studied with fluorescent probes. *J Gen Physiol* 112:145–160
5. Basavappa S, Chartouni V, Kirk K, Prpic V, Ellory JC, Mangel AW (1995) Swelling-induced chloride currents in neuroblastoma cells are calcium dependent. *J Neurosci* 15:3662–3666
6. Beckel JM, Argall AJ, Lim JC, Xia J, Lu W, Coffey EE, Macarak EJ, Shahidullah M, Delamere NA, Zode GS, Sheffield VC et al (2014) Mechanosensitive release of adenosine 5'-triphosphate through pannexin channels and mechanosensitive upregulation of pannexin channels in optic nerve head astrocytes: a mechanism for purinergic involvement in chronic strain. *Glia* 62:1486–1501
7. Bibby KJ, McCulloch CA (1994) Regulation of cell volume and $[\text{Ca}^{2+}]_i$ in attached human fibroblasts responding to anisosmotic buffers. *Am J Phys* 266:C1639–C1649
8. Boudreault F, Grygorczyk R (2004) Cell swelling-induced ATP release is tightly dependent on intracellular calcium elevations. *J Physiol* 561:499–513
9. Boudreault F, Grygorczyk R (2004) Evaluation of rapid volume changes of substrate-adherent cells by conventional microscopy 3D imaging. *J Microsc* 215:302–312
10. Chen B, Nicol G, Cho WK (2007) Role of calcium in volume-activated chloride currents in a mouse cholangiocyte cell line. *J Membr Biol* 215:1–13
11. Civan MM, Coca-Prados M, Peterson-Yantorno K (1994) Pathways signaling the regulatory volume decrease of cultured nonpigmented ciliary epithelial cells. *Invest Ophthalmol Vis Sci* 35:2876–2886
12. Dargan SL, Parker I (2003) Buffer kinetics shape the spatiotemporal patterns of IP_3 -evoked Ca^{2+} signals. *J Physiol* 553:775–788

13. Di CG, Ferrara MA, Miccio L, Merola F, Memmolo P, Ferraro P, Coppola G (2015) Holographic imaging of unlabelled sperm cells for semen analysis: a review. *J Biophotonics* 8:779–789
14. Doroshenko P, Neher E (1992) Volume-sensitive chloride conductance in bovine chromaffin cell membrane. *J Physiol* 449:197–218
15. Farinas J, Verkman AS (1996) Cell volume and plasma membrane osmotic water permeability in epithelial cell layers measured by interferometry. *Biophys J* 71:3511–3522
16. Gong W, Xu H, Shimizu T, Morishima S, Tanabe S, Tachibe T, Uchida S, Sasaki S, Okada Y (2004) CIC-3-independent, PKC-dependent activity of volume-sensitive Cl channel in mouse ventricular cardiomyocytes. *Cell Physiol Biochem* 14:213–224
17. Groulx N, Boudreault F, Orlov SN, Grygorczyk R (2006) Membrane reserves and hypotonic cell swelling. *J Membr Biol* 214:43–56
18. Grygorczyk R, Boudreault F, Platonova A, Orlov SN (2015) Salt and osmosensing: role of cytoplasmic hydrogel. *Pflugers Arch* 467:475–487
19. Guilak F, Erickson GR, Ting-Beall HP (2002) The effects of osmotic stress on the viscoelastic and physical properties of articular chondrocytes. *Biophys J* 82:720–727
20. Hermoso M, Olivero P, Torres R, Riveros A, Quest AF, Stutzin A (2004) Cell volume regulation in response to hypotonicity is impaired in HeLa cells expressing a protein kinase C alpha mutant lacking kinase activity. *J Biol Chem* 279:17681–17689
21. Hoffmann EK, Lambert IH, Pedersen SF (2009) Physiology of cell volume regulation in vertebrates. *Physiol Rev* 89:193–277
22. Hornbeck PV, Zhang B, Murray B, Kornhauser JM, Latham V, Skrzypek E (2015) PhosphoSitePlus, 2014: mutations, PTMs and recalibrations. *Nucleic Acids Res* 43:D512–D520
23. Jorgensen NK, Christensen S, Harbak H, Brown AM, Lambert IH, Hoffmann EK, Simonsen LO (1997) On the role of calcium in the regulatory volume decrease (RVD) response in Ehrlich mouse ascites tumor cells. *J Membr Biol* 157:281–299
24. Kirk J, Kirk K (1994) Inhibition of volume-activated I- and taurine efflux from HeLa cells by P-glycoprotein blockers correlates with calmodulin inhibition. *J Biol Chem* 269:29389–29394
25. Kunzelmann K (2015) TMEM16, LRRC8A, bestrophin: chloride channels controlled by Ca(2+) and cell volume. *Trends Biochem Sci* 40:535–543
26. Liu G, Liu G, Chen H, Borst O, Gawaz M, Vortkamp A, Schreiber R, Kunzelmann K, Lang F (2015) Involvement of Ca2+ activated Cl- Channel Ano6 in platelet activation and apoptosis. *Cell Physiol Biochem* 37:1934–1944
27. Liu W, Xie Y, Ma J, Luo X, Nie P, Zuo Z, Lahrmann U, Zhao Q, Zheng Y, Zhao Y, Xue Y et al (2015) IBS: an illustrator for the presentation and visualization of biological sequences. *Bioinformatics* 31:3359–3361
28. McCarty NA, O'Neil RG (1992) Calcium signaling in cell volume regulation. *Physiol Rev* 72:1037–1061
29. Mola MG, Sparaneo A, Gargano CD, Spray DC, Svelto M, Frigeri A, Scemes E, Nicchia GP (2016) The speed of swelling kinetics modulates cell volume regulation and calcium signaling in astrocytes: a different point of view on the role of aquaporins. *Glia* 64:139–154
30. Mongin AA (2016) Volume-regulated anion channel—a frenemy within the brain. *Pflugers Arch* 468:421–441
31. Mongin AA, Kimelberg HK (2002) ATP potently modulates anion channel-mediated excitatory amino acid release from cultured astrocytes. *Am J Physiol Cell Physiol* 283:C569–C578
32. Mongin AA, Kimelberg HK (2005) ATP regulates anion channel-mediated organic osmolyte release from cultured rat astrocytes via multiple Ca2+-sensitive mechanisms. *Am J Physiol Cell Physiol* 288:C204–C213
33. Morley SM, Dundas SR, James JL, Gupta T, Brown RA, Sexton CJ, Navsaria HA, Leigh IM, Lane EB (1995) Temperature sensitivity of the keratin cytoskeleton and delayed spreading of keratinocyte lines derived from EBS patients. *J Cell Sci* 108(Pt 11):3463–3471
34. O'Connor ER, Kimelberg HK (1993) Role of calcium in astrocyte volume regulation and in the release of ions and amino acids. *J Neurosci* 13:2638–2650
35. Pasantes-Morales H, Morales MS (2000) Influence of calcium on regulatory volume decrease: role of potassium channels. *Nephron* 86:414–427
36. Pedersen SF, Okada Y, Nilius B (2016) Biophysics and physiology of the volume-regulated Anion Channel (VRAC)/volume-sensitive outwardly rectifying anion channel (VSOR). *Pflugers Arch* 468:371–383
37. Pedersen SF, Prenen J, Droogmans G, Hoffmann EK, Nilius B (1998) Separate swelling- and Ca2+-activated anion currents in Ehrlich ascites tumor cells. *J Membr Biol* 163:97–110
38. Platonova A, Boudreault F, Kapilevich LV, Maksimov GV, Ponomarchuk O, Grygorczyk R, Orlov SN (2014) Temperature-induced inactivation of cytoplasmic biogel osmosensing properties is associated with suppression of regulatory volume decrease in A549 cells. *J Membr Biol* 247:571–579
39. Qiu Z, Dubin AE, Mathur J, Tu B, Reddy K, Miraglia LJ, Reinhardt J, Orth AP, Patapoutian A (2014) SWELL1, a plasma membrane protein, is an essential component of volume-regulated anion channel. *Cell* 157:447–458
40. Quiros-Gonzalez I, Sainz RM, Hevia D, Mayo JC (2011) MnSOD drives neuroendocrine differentiation, androgen independence, and cell survival in prostate cancer cells. *Free Radic Biol Med* 50:525–536
41. Rudkouskaya A, Chemoguz A, Haskew-Layton RE, Mongin AA (2008) Two conventional protein kinase C isoforms, alpha and beta I, are involved in the ATP-induced activation of volume-regulated anion channel and glutamate release in cultured astrocytes. *J Neurochem* 105:2260–2270
42. Shen MR, Chou CY, Browning JA, Wilkins RJ, Ellory JC (2001) Human cervical cancer cells use Ca2+ signalling, protein tyrosine phosphorylation and MAP kinase in regulatory volume decrease. *J Physiol* 537:347–362
43. Shen MR, Furla P, Chou CY, Ellory JC (2002) Myosin light chain kinase modulates hypotonicity-induced Ca2+ entry and Cl- channel activity in human cervical cancer cells. *Pflugers Arch* 444:276–285
44. Sirianant L, Wanitchakool P, Ousingasawat J, Benedetto R, Zormpa A, Cabrita I, Schreiber R, Kunzelmann K (2016) Non-essential contribution of LRRC8A to volume regulation. *Pflugers Arch* 468:805–816
45. Sit ST, Manser E (2011) Rho GTPases and their role in organizing the actin cytoskeleton. *J Cell Sci* 124:679–683
46. Souza MM, Boyle RT (2001) A moderate decrease in temperature inhibits the calcium signaling mechanism(s) of the regulatory volume decrease in chick embryo cardiomyocytes. *Braz J Med Biol Res* 34:137–141
47. Speake T, Douglas IJ, Brown PD (1998) The role of calcium in the volume regulation of rat lacrimal acinar cells. *J Membr Biol* 164:283–291
48. Szucs G, Heinke S, Droogmans G, Nilius B (1996) Activation of the volume-sensitive chloride current in vascular endothelial cells requires a permissive intracellular Ca2+ concentration. *Pflugers Arch* 431:467–469
49. Tatur S, Groulx N, Orlov SN, Grygorczyk R (2007) Ca2+ -dependent ATP release from A549 cells involves synergistic autocrine stimulation by co-released uridine nucleotides. *J Physiol* 584:419–435
50. Thul R, Coombes S, Roderick HL, Bootman MD (2012) Subcellular calcium dynamics in a whole-cell model of an atrial myocyte. *Proc Natl Acad Sci U S A* 109:2150–2155

51. Voss FK, Ullrich F, Munch J, Lazarow K, Lutter D, Mah N, Andrade-Navarro MA, von Kries JP, Stauber T, Jentsch TJ (2014) Identification of LRRC8 heteromers as an essential component of the volume-regulated anion channel VRAC. *Science* 344:634–638
52. Yap KL, Kim J, Truong K, Sherman M, Yuan T, Ikura M (2000) Calmodulin target database. *J Struct Funct Genom* 1:8–14
53. Zhou HX, Rivas G, Minton AP (2008) Macromolecular crowding and confinement: biochemical, biophysical, and potential physiological consequences. *Annu Rev Biophys* 37:375–397